

## Interpretation of Microseismicity at the Rotokawa Geothermal Field, 2008 to 2012

Sewell, S. M.<sup>1</sup>, Cumming, W.<sup>2</sup>, Bardsley, C.J.<sup>1</sup>, Winick, J.<sup>1</sup>, Quiniao, J.<sup>1</sup>, Wallis, I.C.<sup>1</sup>, Sherburn, S.<sup>3</sup>, Bourguignon, S.<sup>4</sup>, Bannister, S<sup>4</sup>

<sup>1</sup>Mighty River Power Limited, 283 Vaughan Road, Rotorua 3010

<sup>2</sup>Cumming Geoscience, 4728 Shade Tree Lane, Santa Rosa CA 95405-7841

<sup>3</sup>GNS Science, Wairakei, Private Bag 2000 Taupo 3352

<sup>4</sup>GNS Science, Avalon, PO Box 30-368, Lower Hutt 5040

[Steven.Sewell@mightyriver.co.nz](mailto:Steven.Sewell@mightyriver.co.nz)

**Keywords:** Rotokawa, microseismic, geophysics

### ABSTRACT

At the Rotokawa Geothermal Field, the integrated interpretation of microseismic (MEQ) data with other geoscience and reservoir engineering data has helped identify and constrain important elements of the reservoir model, including a major structure that likely influences reservoir fluid flow. MEQ monitoring began when injection moved to deeper wells in 2006, and an 8-10 seismometer array has been operating continuously since mid-2008. To meet goals for characterizing large-scale reservoir permeability structure and tracking the path of injection, two lines of investigation were pursued; 1) obtaining accurate MEQ locations, and 2) inferring reservoir properties by comparing the MEQ locations and timing with relevant reservoir data. Manual phase picking and double-difference relative re-location was used to significantly improve location accuracy from initial automated locations. These more accurate locations were used to support the use of 4D visualization tools to interpret MEQ patterns in space and time with respect to the integrated geoscience and reservoir engineering data sets.

Correlation of the MEQs with changes in well flows, pressure and temperature data has been particularly important to understanding likely causes of the MEQs and their implications for reservoir properties. Most MEQs at Rotokawa appear to be triggered by injection cooling and field-wide pressure transients, although other mechanisms are possible. Many MEQs occur in swarms of >10 events/day along a linear, northeast trending structure – the Central Field Fault (CFF). The majority of the remaining MEQs are clustered on the southeast side of this structure that separates injection wells to the southeast and production wells to the northwest. The location and timing of the MEQs relative to major changes in production and injection are consistent with other geoscience data sets suggesting that the northeast trending structure acts as a barrier to fluid flow across strike and a zone of enhanced permeability along strike. This structure and the effective base of the reservoir permeability are the main features interpreted from the MEQ data that have been incorporated into the Rotokawa conceptual and numerical models, which are used to guide field management.

### 1. INTRODUCTION

The Rotokawa geothermal field is located within the Taupo Volcanic Zone (TVZ) a center of active rifting in the North Island of New Zealand (Figure 1). The resource potential of the Rotokawa field was first identified from numerous surface thermal features, including acid sulphate fumaroles, steaming ground and bi-carbonate springs, and from resistivity surveys (Schlumberger soundings). Exploratory drilling undertaken from 1965 to 1986 by the New Zealand government (RK1 – RK6, RK8) confirmed the presence of a large, high temperature (>300 °C) geothermal resource.

Electricity generation of 24 MWe began on the field in 1997 with the installation of the binary, Rotokawa plant. Production was initially from wells RK5 and RK9 with shallow injection at about 500 to 1000 m depth into RK1, RK11, and RK12. In 2000, Mighty River Power and Tauhara North No. 2 Trust formed the Rotokawa Joint Venture and generation was subsequently expanded to 34 MWe. Following analyses of well results and 1D/2D MT-TDEM resistivity imaging, shallow injection was shifted to deeper zones at ~1000-3000m depth in RK16 and RK18 in 2005. This shift from shallow to deep injection prompted the initial deployment of seismometers at Rotokawa.

In 2007, resource consents were obtained for a further development at Rotokawa, supported by conceptual and numerical modeling of the field based on production history (Rotokawa plant) and well results up to RK18 (Bowyer & Holt, 2010). The Nga Awa Purua (NAP) development began in 2008 with the drilling of wells RK19 to RK30 and construction of a 140 MWe, triple-flash plant which was commissioned in early 2010. Since then make-up production wells RK32 and RK33 have been drilled.

The shift of injection from shallow to deep wells prompted an initial deployment of a single seismometer in July, 2005 to assess seismicity rates in the field. More than 350 MEQs of magnitude ML -0.5 to 2.5 were detected in ~1 month, justifying expansion of the monitoring to a ten seismometer network in April-August, 2006. This network was aimed at more accurately locating and characterizing the seismicity. The 2006 seismometer deployment revealed an approximate NE-SW MEQ trend extending over 1-2 km from the RK16-RK18 injection area (Bannister et al, 2008). Following this, a long-term seismic network was installed, initially consisting of 8 portable seismometers in July, 2008 with a further two seismometers installed in October, 2008. This ten seismometer array has operated almost continuously since then, with adjustments to the array geometry to ensure accurate

hypocenter locations in the injection and production areas while adapting to changes in the generally high noise levels related to the geothermal power plant facilities.

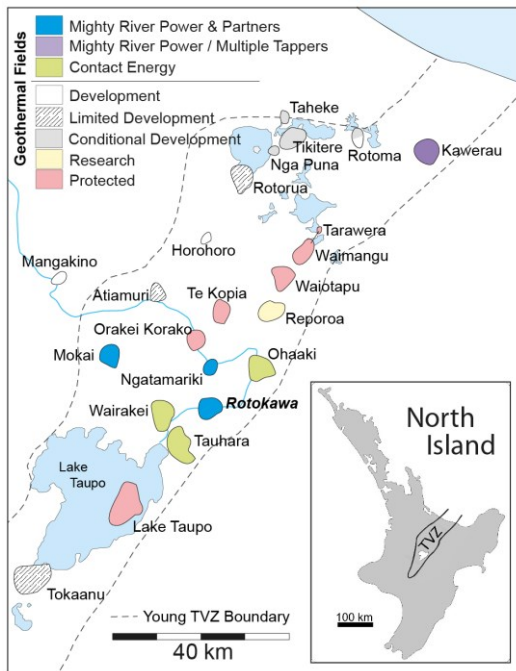


**Figure 1. Location of known geothermal fields in the Taupo Volcanic Zone (TVZ) on the north island of New Zealand as identified by Schlumberger resistivity surveys (Bibby et al., 1995). The Rotokawa field (bold) is approximately 12 km NE of Taupo, 10 km east of Wairakei geothermal field and 10 km south of the Ngatamariki geothermal field.**

Throughout the microseismic monitoring, use of manual re-picking of P and S phases combined with double-difference relative relocation (TomoDD, Zhang and Thurber, 2003) has been essential to obtaining event locations accurate enough to provide useful interpretations for the reservoir model. Sherburn et al. (2013) details the acquisition and processing methods used at Rotokawa to ensure sufficient event detection and hypocenter location accuracy. They estimate the absolute uncertainty of events located using these methods to be  $<50$  m horizontally and approximately  $+/- 500$  m vertically. Although manual re-picking has been essential for obtaining accurate locations, it is expected that improved automated picking techniques when combined with double-difference relative relocation could achieve similar results.

From experience at other operating, conventional, geothermal fields (e.g., Mossop, 2003), it seemed likely that stress related to rock cooling and contraction in response to injection of  $<140$  °C water into a  $>300$  °C, deep ( $>1000$  m) reservoir at Rotokawa might induce small, but potentially detectable MEQs on existing fractures. Because the flash technology employed in the NAP development would result in roughly 25% net reservoir voidage, a gradual net pressure decline was expected throughout the permeable deep reservoir. It was therefore thought that pressure increase would not be a primary cause of MEQ activity, although small, local pressure increases around injection wells may cause some MEQ activity. However, MEQ's related to large increases in pressure, similar to those observed during Enhanced Geothermal System (EGS) well stimulation activities (e.g., Majer et al. 2007), were very unlikely to occur at Rotokawa because operating injection well pressures would be far below the fracture gradient (i.e., below the magnitude of  $S_{h\min}$ ;  $S_v > S_{h\max} > S_{h\min}$  at Rotokawa). Minor compaction associated with gradual pressure decline and changes in fluid compressibility due to boiling might eventually change stress near fractures enough to induce MEQs in a pattern generally shallower and more diffuse than injection-related MEQs (e.g., Segall, 1989). The timing of the MEQs associated with cooling and compaction might be influenced when small fractures stressed close to failure are perturbed by transient pressure/stress variations caused by changes in field operations or by distant earthquakes (e.g., Hanano, 1995; and Hill et al., 1993). Based on these physical models for MEQ occurrence, the initial objectives of the Rotokawa MEQ monitoring included; improving field management by tracing injection movement, detecting major pathways and barriers to flow, and characterizing the base of the permeable reservoir reached by injection.

In this paper, a review of the MEQ monitoring and data analysis at Rotokawa supports a summary of the MEQ hypocenter data set used in the space-time analysis. The space and time correlation of the MEQs with the production and injection history and integration with other geoscience datasets support conceptual models for injection flow and reservoir permeability. In particular, these models support the interpretation of a fault (referred to herein as the Central Field Fault (CFF)) that likely acts as both a barrier and a conduit. These interpretations have been implemented as important components of the current Rotokawa conceptual and reservoir simulation models.

## 2. 4D MICROSEISMIC INTERPRETATION

### 2.1 Major Changes in MEQ Activity with Time

#### 2.1.1 Pre-NAP; 2006 - February, 2010

Over the monitoring period, at least four significant changes in the location and/or rate of microseismic activity have been observed at Rotokawa, all of which are correlated with changes in the location and rate of injection. Deep injection commenced in 2005 into RK18 and RK16 and continued until October, 2008. Intermittent monitoring over this period revealed a broad NE-SW trending pattern of seismicity extending from the RK18-16 area towards RK13 (Figure 2). A tracer test conducted in 2006 showed large and rapid tracer returns from RK18 to RK17 with delayed returns to RK13 along an inferred structural path (Winick, 2013). It appears likely that at least part of the early MEQ activity is associated with the movement of injectate along this structure.

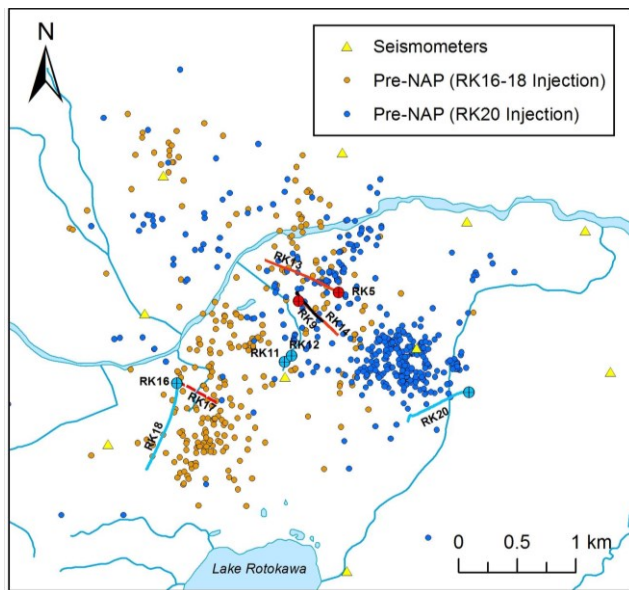


**Figure 2. MEQ pattern from April 2006 to August, 2006 and from July, 2008 to Feb, 2010. A shift in the location of MEQ activity occurs coincident with injection shifting from RK16 & RK18 (orange dots) to RK20 (dark blue dots) in October, 2008. Production wells are in red and injection wells in blue.**

Partly as a result of the 2006 tracer test, the production-injection strategy was revised and injection was relocated to RK20 in the southeastern part of the field in October, 2008. This also shifted the location of MEQ activity to the southeast, slightly offset from the RK20 well track towards the production wells operating at that time (RK5, RK13 and RK14, Figure 2). No linear features that might indicate structures were prominent in the MEQ pattern during this period of injection into RK20.

#### 2.1.2 Post-NAP; February, 2010 – December, 2012

An almost three-fold increase in total deep injection within the field, from  $\sim$ 650 t/h to  $\sim$ 1850 t/h, occurred in February, 2010 with the commissioning of the NAP power station (Figure 3). This more than doubled the average rate of seismicity within the field from  $\sim$ 1 to  $\sim$ 2 events per day.

Over the first year of NAP operation, a more prominent pattern began to emerge from the MEQ locations. The majority of seismicity was located in a 1000 m x 750 m x 1500m depth box, starting just NE of the injection well feed zones and extending towards production (Figure 4). A prominent NE-SW trend appeared to be marking the boundary between a dense cluster of MEQs near the injection wells and a zone with sparse MEQs near the production area to the NW. It appeared that this NE-SW trend was associated with a major fault, the CFF, which had been previously inferred to exist between the injection and production areas from vertical offset in the greywacke and Rotokawa Andesite and a NE-SW alignment of surface thermal features (e.g., Nairn, 1984, Browne et al., 1992; Bowyer & Holt, 2010, Wallis et al. 2013).

Although RK21 alone accounted for over half of the total NAP injection capacity for most of 2010 (Figure 3), very little seismicity was located close to this well. In late December, 2010 brine injection from NAP ( $\sim$ 1100 t/h) was shifted from RK21 into RK24. This shift in injection appears to be correlated with a shift in the general location of seismicity within the field (Figure 4), although the new MEQ activity remains similarly confined to the SE of the NE-SW trending CFF.

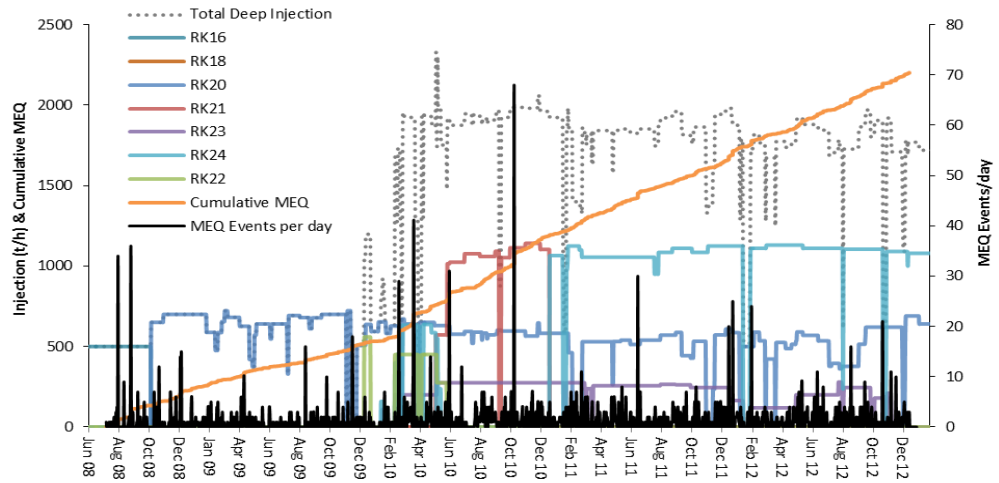


**Figure 3.** Cumulative MEQ events and MEQ events per day from July, 2008 to December, 2012 and a simplified deep injection history. A noticeable change in the rate of MEQ activity is coincident with a significant increase in deep injection in February, 2010. Swarm-like activity (>10-15 MEQ events/day) occurs throughout the monitoring period and appears to be sometimes associated with major changes in production and injection (e.g., start of RK21 around June, 2010). The location of swarms of greater than 15 events per day is plotted in Figure 5.

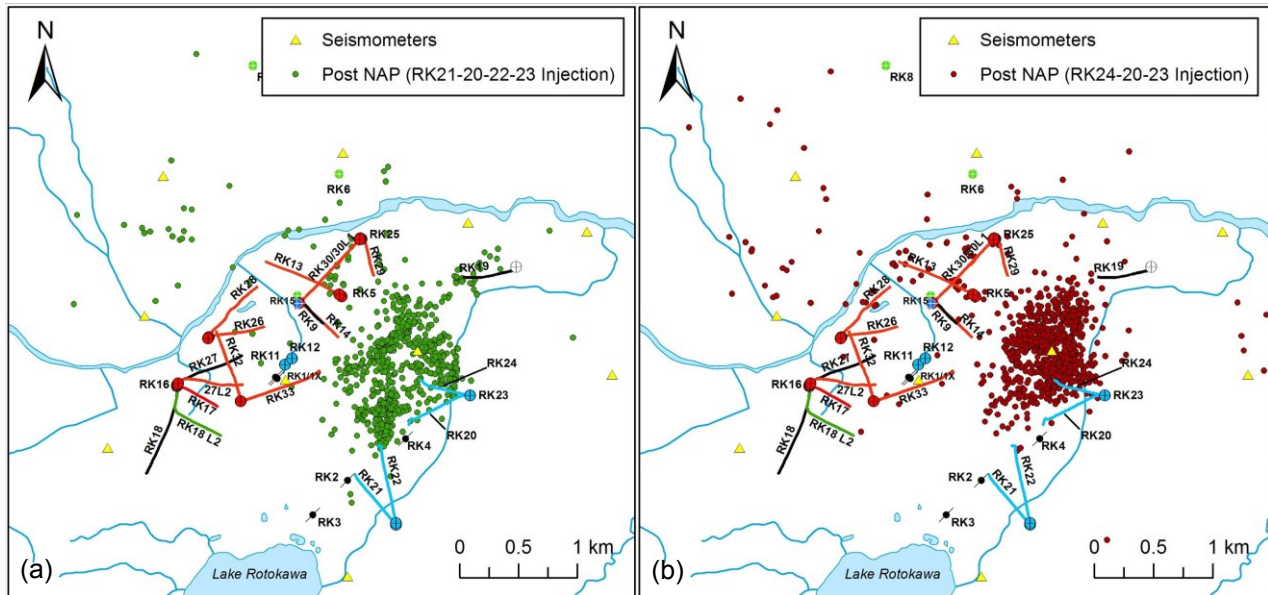


**Figure 4.** MEQ locations (a) from February, 2010 to December 2010 and (b) December, 2010 to December, 2012. A shift in the location of MEQ activity to the northwest is coincident with a large shift of injection from RK21 into RK24. Production wells are red, injection wells are blue, monitoring wells are green and abandoned wells are black.

## 2.2 ‘Swarm’ Activity

Although the long-term average rate of MEQs at Rotokawa is ~1-2 MEQ events per day, there have been many days where the number of events has been significantly above this rate (Figure 3). Between July, 2008 and December, 2012 there have been around fifteen days with >15 events and six days with >10 events of sufficient quality to be relocated. The majority of MEQs within these groups or “swarms” occur within minutes of each other, and do not appear to show the characteristic pattern of aftershocks in magnitude, time or space.

Since injection was moved to the south-east of the field in October, 2008 (RK20-24), the majority of this swarm activity has occurred along or confined to the SE of the same NE-SW trending structure (CFF) located approximately half way between the production and injection wells (Figure 5). The bulk of the remaining MEQ activity during southern injection has been along or southeast of this linear feature, closer to the injection wells. The larger magnitude events (magnitudes 2-3.5) since October, 2008 have also occurred in the same area as the swarm activity.

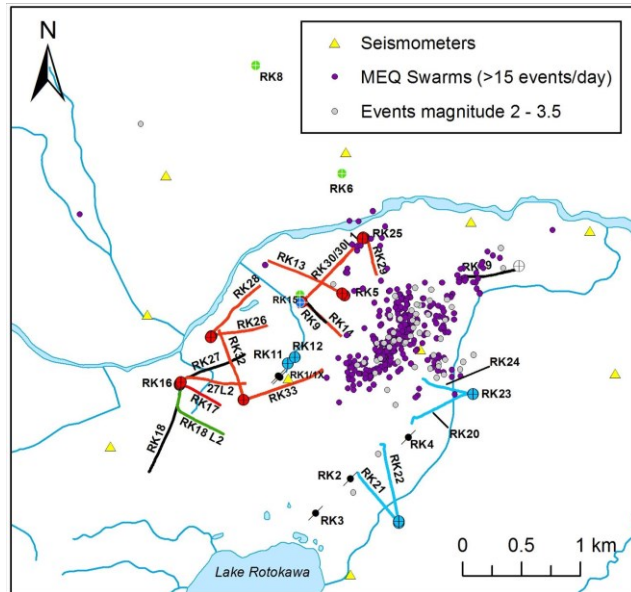


**Figure 5. MEQ swarms of more than 15 events per day since injection commenced in the southern part of the field (since October, 2008).**

### 2.3 MEQ Mechanisms at Rotokawa

The majority of fractures imaged using acoustic logs from about 1000 to 2500 m depth in the volcanic formations at Rotokawa are at orientations favorable for reactivation in the modern stress field, likely because they formed in a stress field similar to the present one ( $S_v = \sigma_1$  and  $S_{Hmax}$  has a NE-SW orientation; also c.f., Davidson et al. 2012). The south-eastern injection wells terminate in the meta-sedimentary sandstone and siltstone formation, often generically called greywacke basement, that underlies the volcanic formations. These meta-sediments typically contain numerous pre-existing fractures at all orientations, reflective of the long structural history of these Mesozoic-age rocks. The fractures are commonly either open or contain calcite fills with low cohesive strength. It follows that there are numerous pre-existing planes of weakness with low cohesive strength in the Rotokawa reservoir rocks, many of which are likely to be critically stressed and optimally orientated for reactivation with minor stress-field perturbation. At Rotokawa it appears that temperature change is the main cause of stress-field perturbation; however pressure effects are also apparent.

Consistent with initial expectations, it appears likely that most of the MEQs near the permeable zones in injection wells occur due to stresses related to contraction of rock due to injection cooling. Since the start of NAP production, injection area pressure change has been small to negligible, with any local pressure increase associated with injection offset by the overall net voidage (extracted fluid minus injection) of the reservoir (Quiniao et al., 2013, Figure 7). Where positive well head pressures have been measured, they have not exceeded 15 bar, and injection pressures have been well below the measured fracture gradient ( $S_{Hmax}$  magnitude: Davidson et al. 2012). However, the temperature difference between the natural state reservoir (initial measured temperatures in RK20-24 of 330-340 °C) and the injected fluid (80-130 °C) is large and the thermal stresses associated with this are likely enough to account for most of the seismicity (e.g., Mossop, 2003, Dempsey, et al. 2013). Well bore image log observations of limited compressive and extensive tensile failure in geothermal wells due to thermal stresses around the wellbore (Fernasez-Ibanez et al. 2009 & Halwa et al. 2013) and the improvement of well permeability at pressures below the fracture gradient through the injection of fluids cooler than the reservoir (Grant et al. 2013 & Dempsey et al. 2013) also support the hypothesis that thermal stress is a key process creating MEQs at Rotokawa. However, local pressure increases near the injectors may also be sufficient to induce slip on critically stressed, pre-existing fractures and changes in rock cohesive strength through mineral deposition and dissolution by injected fluids may also be a significant process in triggering MEQs at Rotokawa (e.g. neutralization reactions of the mildly acidic injection fluid with calcite fractures).

Some of the MEQ swarms appear to occur soon (within days) after major changes in production-injection (e.g., start of RK24 in Feb 2010, start of RK21 in June, 2010; Figure 3). Other swarms do not have an obvious correlation with variations in production or injection, occurring sporadically over time. From the apparent time correlation of some swarms with production-injection changes, it appears that large-scale, transient pressure changes within the reservoir may trigger some of the MEQ swarms at Rotokawa. These swarms are unlikely to be related to cooling stresses because the events occur ~500m from the injection zones in the wells. Modeling and observations indicate that significant cooling is unlikely to take place within a few days at such lateral distances. On the other hand, pressure transients can propagate such distances in shorter times. Similar swarm activity has been correlated with large changes in production-injection such as a field shut-in for maintenance at other geothermal fields (e.g., Kakkonda in Japan, Hanano, 1995).

Five MEQ swarms containing >15 events per day have been observed since continuous downhole pressure monitoring was installed in RK22 in the south-east injection area in late 2011 (Figure 6). Comparison of the swarms to the downhole pressure in RK22 appears to confirm that two of the swarms occur during transient pressure changes in the injection area. These swarms appear to occur within a few days of major changes in injection rates and resulting transient changes in injection area pressure (as measured

by RK22). Interestingly, the swarm in January, 2012 occurs within a few days of injection starting (i.e. whilst pressure in RK22 is increasing) whereas the swarm in October, 2012 appears to occur within a few days of injection switching off (i.e. whilst pressure in RK22 is decreasing). It is clear in the comparison of MEQ rates with RK22 downhole pressure that the swarms are not always associated with transient pressure changes in the injection area and there must be other mechanisms that trigger the swarm activity (e.g., long period change in stress due to cooling contraction, tectonic movement, remote triggering by distant large earthquakes, etc). A more complete set of measurements related to potential causes (e.g., pressure in other wells, broad band seismometers capable of detecting distant earthquakes) and a longer period of measurement are needed to better establish causes of the MEQ swarms.

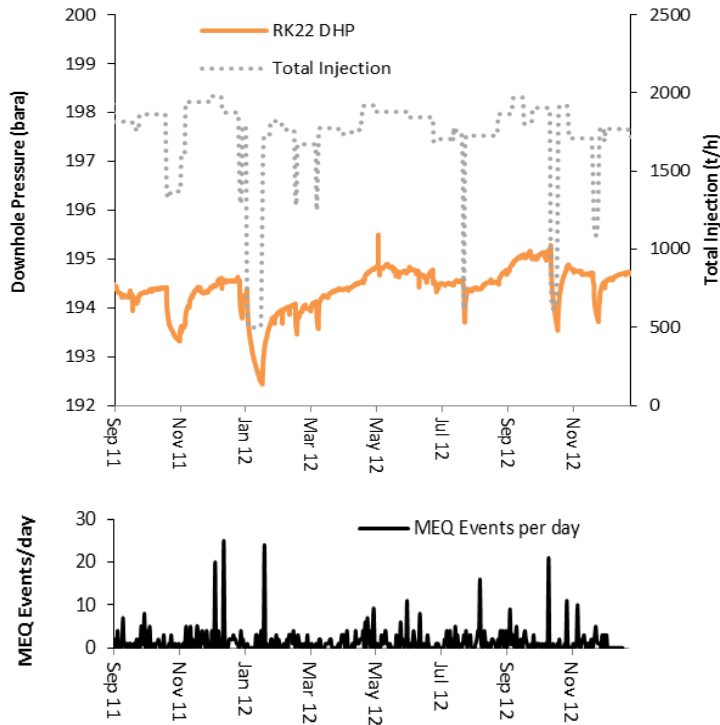


**Figure 6. Comparison of MEQ events per day to downhole pressure monitoring in RK22 (at -2200 m elevation) and total deep injection. Two swarms, in January and October, 2012 appear to be associated with transient pressure change in the injection area. Other swarms however do not appear to have a correlation with pressure change in the injection area.**

It remains unclear why no seismicity occurred around injection feedzones in RK21 whilst it was injecting  $\sim$ 1100 t/h of 130 °C brine from June – December, 2010. A variety of mechanisms have been proposed that might account for the lack of MEQs including; differences in stress state and formation properties (e.g. rock cohesive strength), a smaller cooled zone along a more focused, high permeability, flow path with lower initial stress, and a more subdued pressure response in a high permeability zone better connected to production. However, there is insufficient evidence at this point to support a preferred model.

### 3. USE OF MICROSEISMICITY IN RESERVOIR CONCEPTUAL AND NUMERICAL MODELS AND FIELD MANAGEMENT

#### 3.1 Central Field Fault: Barrier Across Strike, Conduit Along Strike

The observation that the majority of the MEQs do not extend across the CFF toward the production zone suggests that the fault acts as a barrier to injection fluid flow across its strike (i.e., NW-SE direction; Figure 7). Current reservoir tracer results indicate relatively slow and relatively low percentage returns of injection to production (60-100 day first arrivals from current injection to production; Winick, 2012). These results are significantly different from a previous tracer test in 2006 when injection and production were oriented along the NE-SW structural trend (first-arrivals within several days to weeks from RK18 to RK17 and RK13 respectively). Changes in reservoir pressure since NAP commissioning also suggest that the fault may act to limit pressure support to the production area from injection. Large pressure drops (up to 45 bar) have been observed in the production area, larger than would be expected in a reservoir with 75% in-field injection (Quiniao et al., 2013). However, net long-term, pressure change in the injection area has remained at approximately zero (Quiniao et al., 2013), so it does not appear that pressure is building-up behind the fault. These observations combined with the tracer results suggests the fault acts to significantly slow or divert the direct return of injection rather than to completely block its return. Faults acting as barriers that act to compartmentalize geothermal reservoirs have been noted elsewhere (e.g., the Awibengkok reservoir in Indonesia, Stimac et al, 2008).

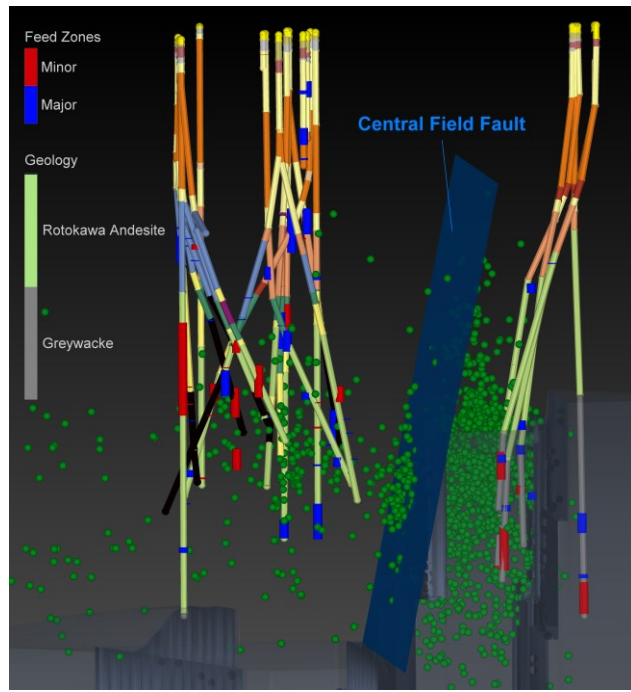


**Figure 7. MEQ's from July, 2008 to December, 2012, the Central Field Fault and greywacke. Vertical displacement in the greywacke across the fault is ~500m.**

Comparison of the location of the fault with other geoscience datasets suggests that the fault is also associated with enhanced permeability along strike. The projected surface trace of the CFF, as constrained by the MEQ, appears to align a number of surface thermal features including Lake Rotokawa, several hydrothermal eruption craters and the Rotokawa Fumarole (Figure 8). Gas geothermometry ( $\text{CO}_2/\text{Ar}-\text{H}_2/\text{Ar}$ ) of the Rotokawa Fumarole indicates that it is sourced directly, from the deep,  $>300$  °C liquid reservoir with relatively minor intervening processes. The fumarole gas chemistries are also very similar in composition with gases obtained from a flow test of RK4 (N2-He-Ar; Hedenquist et. al, 1988). This suggests the fumarole is sourced directly from the deep reservoir without significant residence time for re-equilibration in the overlying intermediate aquifer (Winick, 2011). The approximate surface trace of the fault also coincides with the area at the boiling point in its natural state from 100 to 1000 m depth, which extends in a relatively broad area from RK2-RK4 to RK1/11/12 (Sewell et al., 2012). These observations suggest that the fault may act as the main permeable connection between the deep reservoir and the intermediate aquifer, although there are likely other permeable connections within the broader boiling point for depth region.

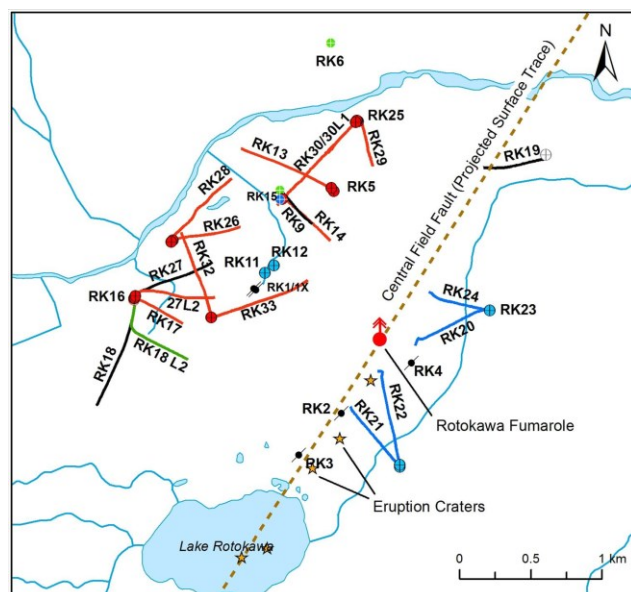


**Figure 8. Location of the projected surface trace of the Central Field Fault in relation to the Rotokawa Fumarole and several hydrothermal eruption craters.**

The interpretation of the CFF as a barrier across strike and a conduit along strike has been important for numerical modeling and field management. The CFF appears to impede the flow of injection back to production, mitigating production enthalpy decline due to injection return. Although indications of injection chemical breakthrough to production have been observed (Winick, 2013), no related declines in well temperatures or production enthalpy have been observed to-date. The location of the fault inferred from the MEQ locations has been used to assist with production make-up well targeting. The fault has been included in the reservoir numerical model as a reduction in permeability across its strike and increased permeability along strike (Hernandez et al, 2015).

### 3.2 Base of Permeability in the Injection Area

Permeable zones that account for most of the flow in the deep injection wells range from -1500 m to -3000 m elevation. Most MEQs also occur in the range of -1500 m to -3000 m elevation with relatively few events occurring below -3000 m and only a few occurring below -3500 m (Figure 9). Using the interpretation that the majority of the MEQs are triggered by thermal stresses due to cooling, we therefore inferred that most of the injected fluid does not sink to great depth below the injection feed zones. This implies either, that vertical permeability is generally low below the injection zones within the injection area and/or that injection fluid is re-heated relatively quickly once in the reservoir. In either case, the base of the MEQ activity is indicating the 'effective' base of the reservoir (i.e. the base of the volume of rock that is being cooled by injection).

Although the MEQs do not appear to extend much below injection points, there is significant uncertainty in the depth estimates for these events. Depth uncertainty is estimated to be +/- 500 m, due mostly to uncertainty in the velocity model used to locate the earthquakes (Sherburn et al, 2013). Velocity above ~1000 m is particularly uncertain as it is poorly resolved by tomography, the current basis of the velocity model at Rotokawa. Performing a check-shot survey to directly measure velocities shallower than 1000 m depth would significantly reduce this uncertainty.

Based mostly on the observation that the MEQs do not appear to extend below injection points, whilst taking into account likely uncertainty in depth, the permeability in the Rotokawa numerical model has been lowered between -3000m and -4000m elevation (Hernandez et al, 2015).

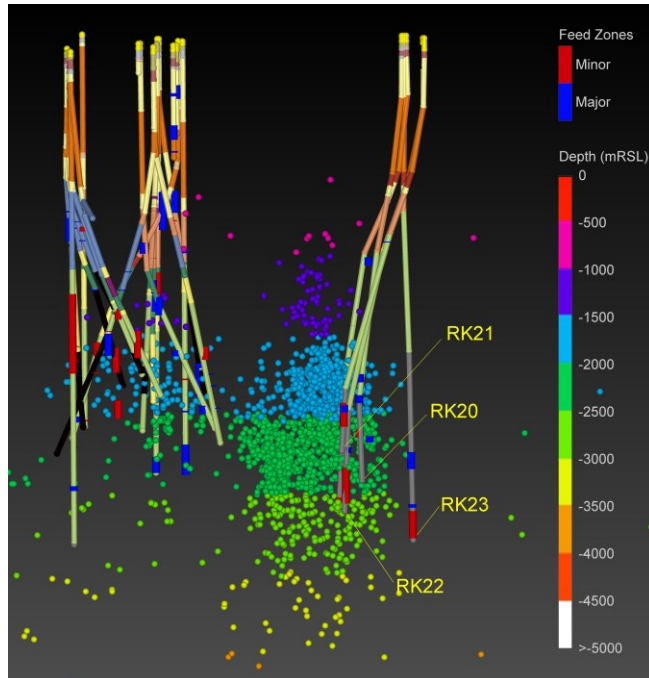


**Figure 9. MEQ with depth in relation to injection feedzones (blue and red bars on well tracks). The majority of MEQ activity has been at the same depths as injection feedzones (-1500m to -3000m elevation). Relatively few events have occurred below the injection feeds and from this, vertical permeability in the injection area is inferred to be relatively low.**

## CONCLUSION

Microseismic monitoring has usefully constrained the pattern of injection flow at Rotokawa and characterised a major structure that likely influences reservoir hydrology. Detailed correlation of the MEQs with operational data (production/injection locations and flows) over time has been important to the interpretation. This was supported by further conceptual integration with other geoscience datasets, particularly the geology, geochemistry, natural state temperatures, and MT resistivity. The permeability pattern inferred from the MEQs has been integrated into the conceptual and numerical models of the Rotokawa reservoir.

A major NE-SW trending structure, the Central Field Fault (CFF), bounds the extension of the MEQs from the injection to the production area, and appears to act as a barrier to flow across its strike in a manner consistent with initial tracer observations.

Swarm-like activity (>10-15 events per day) also appears to occur along the CFF and may be triggered by field-wide pressure transients associated with major changes in production and injection. Based on geology, thermodynamics and geochemistry, this fault also appears to be a zone of enhanced permeability along its strike, at least at depths shallower than 1500 m. The fault acting as a barrier across its strike and a conduit along strike has been included in the reservoir conceptual and numerical models and has assisted with production well targeting and the field development strategy.

The majority of MEQ activity occurs over the same depth range as the permeable zones in the injection wells (-1500m to -3000m). This implies either, that vertical permeability is generally low below the injection zones or that injection fluid is re-heated relatively quickly once in the reservoir.

Future work will likely focus on further understanding likely MEQ triggering mechanisms, particularly the causes of the swarm activity within the field and the absence of seismicity near RK21. This will likely include coupled reservoir and geomechanical numerical modelling (that accounts for thermal stresses) to establish causal, as well as correlation-based, interpretations of the MEQs.

## ACKNOWLEDGEMENTS

The authors wish to sincerely thank the Rotokawa Joint Venture (Mighty River Power Ltd and Tauhara North No.2 Trust) for permission to publish these results.

## REFERENCES

Bannister, S.; Sherburn, S.; Powell, T.; Bowyer, D.. Microearthquakes at the Rotokawa Geothermal Field, New Zealand. *Geothermal Resources Council Transactions*. (2008).

Bibby, H.M., Caldwell, G.T., Davey, F.J., & Wenn, T.H.. Geophysical evidence on the structure of the Taupo Volcanic Zone and its hydrothermal circulation. *Journal of Volcanology and Geothermal Research* 68: pp29-58. (1995).

Bowyer, D. and Holt, R.. Case Study: Development of a numerical model by a multi-disciplinary approach, Rotokawa Geothermal Field, New Zealand. *Proceedings World Geothermal Congress 2010*, Bali, Indonesia. (2010).

Browne, P. R. L., Graham, I. J., Parker, R. J., Wood, C. P.. Subsurface andesite lavas and plutonic rocks in the Rotokawa and Ngatamariki geothermal systems, Taupo Volcanic Zone, New Zealand. *Journal of Volcanology and Geothermal Research*, 51, pp199-215. (1992).

Davidson, J., Siratovich, P., Wallis, I., Gravley, D., McNamara, D.. Quantifying the stress distribution at the Rotokawa Geothermal Field, New Zealand. *Proceedings of the New Zealand Geothermal Workshop*. (2012).

Dempsey, D., Clearwater, J., Kelar, S. & Wallis, I., Validation of a coupled thermal-hydrological-mechanical model though a comparative study of shear stimulation in two geothermal fields: Desert Peak, Nevada, USA and Ngatamariki, New Zealand. (2013).

Fernandez-Ibanez, F., Castillo, D., Wyborn, D. & Hindle, D.. Benefits of HT-hostile environments on wellbore stability: a case study from geothermal fields in central Australia. *Proceedings of the Indonesian Petroleum Association 33rd Annual Convention and Exhibition*, May 2009. (2009).

Grant, M. A., Clearwater, J., Quiniao, J., Bixley, P. F., Le Brun, M.. Thermal stimulation of geothermal wells: a review of field data. *Proceedings Thirty-Eighth Workshop on Geothermal Reservoir Engineering*. Stanford University, California. (2013).

Halwa, L., Wallis, I.C., & Torres Lozada, G.. Geological analysis of the volcanic subsurface using resistivity-type borehole images in the Ngatamariki Geothermal Field, New Zealand. (2013).

Hanano, M.. Hydrothermal Convection System of the Kakkonda Geothermal Field, Japan. *Proceedings World Geothermal Congress* (1995).

Hedenquist, J. W., Mroczek, E. K., Giggenbach, W. F.. Geochemistry of the Rotokawa Geothermal System: Summary of Data, Interpretation and Appraisal for Energy Development. DSIR Chemistry Division Technical Note 88/6. (1988).

Hernandez, D., Clearwater, J., Burnell, J., Franz, P., Azwar, L., Marsh, A.. Update on the Modeling of the Rotokawa Geothermal System: 2010 – 2014. *Proceedings of the World Geothermal Congress* (2015).

Hill, D.P., P.A. Reasenberg, A. Michael, W.J. Arabaz, G. Beroza, D. Brumbaugh, J.N. Brune, R. Castro, S. Davis, D. de Polo, W.L. Ellsworth, J. Gomberg, S. Harmsen, L. House, S.M. Jackson, M.J.S. Johnston, L. Jones, R. Keller, S. Malone, L. Munguia, S. Nava, J.C. Pechmann, A. Sanford, R.W. Simpson, R.B. Smith, M. Stark, M. Stickney, A. Vidal, S. Walter, V. Wong, and J. Zollweg.. Seismicity remotely triggered by the magnitude 7.3 Landers, California, earthquake, *Science* 260, 1617–1622 (1993).

Majer, E.L., Baria, R., Stark, M., Oates, S., Bommer, J., Smith, B., and Asanuma, H., Induced seismicity associated with enhanced geothermal systems: *Geothermics*, v. 36, p. 185-222. (2007).

Majer, E. L., Peterson, J. E.. The impact of injection on seismicity at the Geysers, California Geothermal Field. *International Journal of Rock Mechanics & Mining Sciences*, 44, pp 1079-1090. (2007).

Mossop, A.. Seismicity, subsidence and strain at The Geysers Geothermal Field. PhD Dissertation. Stanford University pp. 180. (2003).

Nairn, I. A.. Stratigraphy of RK5 to 2654m. Report to Ministry of Works and Development. (1984).

Quiniao, J., Sirad-Azwar, L., Clearwater, J., Hoepfinger, V., Le Brun, M., Bardsley, C.. Analyses and modeling of reservoir pressure changes to interpret Rotokawa Geothermal Field response to Nga Awa Purua Power Station operation. Proceedings Thirty-Eighth Workshop on Geothermal Reservoir Engineering. Stanford University, California. (2013).

Segall, P.. Earthquakes triggered by fluid extraction. *Geology*, 17-10, 942-946. (1989).

Sewell, S. M., Cumming, W. B., Sirad-Azwar, L., Bardsley, C.. Integrated MT and natural state temperature interpretation for a conceptual model supporting reservoir numerical modeling and well targeting at the Rotokawa Geothermal Field, New Zealand. Proceedings Thirty-Seventh Workshop on Geothermal Reservoir Engineering. Stanford University, California. (2012).

Sherburn, S., Bourguignon, S., Bannister, S., Sewell, S., Cumming, W., Bardsley, C., Winick, J., Quiniao, J., Wallis, I.. Microseismicity at Rotokawa Geothermal Field, 2008 to 2012. (2013).

Stimac, J., Nordquist, G., Suminar, A., Sirad-Azwar, L.. An overview of the Awibengkok geothermal system, Indonesia. *Geothermics*, 37, pp 300-331. (2008).

Wallis, I.C., Bardsley, C.J., Powell, T.S., Rowland, J.V. & O'Brien, J.M.. A structural model for the Rotokawa Geothermal Field, New Zealand. (2013).

Winick, J., Powell T, Mroczek, E.. The Natural-state geochemistry of the Rotokawa Reservoir. Proceedings of the New Zealand Geothermal Workshop (2011).

Winick, J.. Natural-state geochemistry of the Rotokawa deep reservoir. Unpublished MRP report. (2011).

Winick, J.. Rotokawa reservoir, steamfield and process geochemistry. Unpublished MRP report. (2013).

Zhang, H., and C.H. Thurber.. Double-difference tomography: method and application to the Hayward fault, California, *Bull. Seismol. Soc. Am.*, 93 1875, (2003).